IEEE Photonics Journal
An IEEE Photonics Society Publication

Optofluidic Chip of a Single-Mode Fiber Variable Optical Attenuator

Volume 9, Number 2, April 2017

Jing Wan
Fenglan Xue
Boyu Chen
Han Cao
Minling Du
Fangren Hu

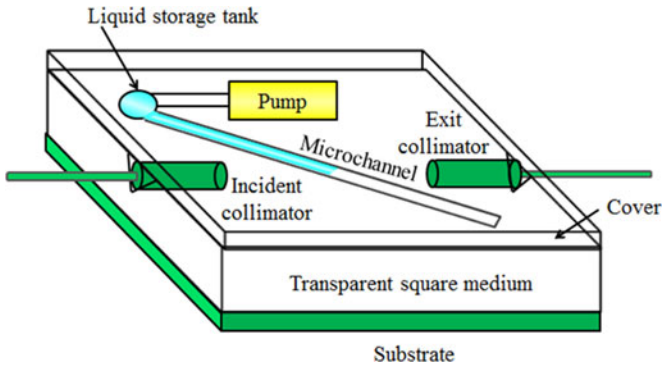

DOI: 10.1109/JPHOT.2017.2672639
1943-0655 © 2017 IEEE

Optofluidic Chip of a Single-Mode Fiber Variable Optical Attenuator

Jing Wan, Fenglan Xue, Boyu Chen, Han Cao, Minling Du, and Fangren Hu

School of Optoelectronic Engineering, Nanjing University of Posts and Telecommunications, Nanjing 210023, China

DOI:10.1109/JPHOT.2017.2672639

Manuscript received January 6, 2017; revised February 8, 2017; accepted February 16, 2017. Date of publication February 22, 2017; date of current version March 22, 2017. This work was supported in part by the National Natural Science Foundation of China under Grant 61574080 and Grant 61274121 and in part by Postgraduate Innovative Projects of Jiangsu Province (SJZZ16_0146). Corresponding author: J. Wan (e-mail: wanj@njupt.edu.cn).

Abstract: An optofluidic chip of the single-mode fiber variable optical attenuator (VOA) is proposed. This chip has a simple structure, and it utilizes microfluid and air to regulate the optical attenuation, where air acts as a shutter. Here, the single-mode characteristics of the VOA chip are discussed at 1310 nm and 1550 nm. The experiment results indicate that it is feasible to regulate optical attenuation using the proposed chip. The VOA with this chip has a large optical attenuation range (82 dB) and a very wide operation waveband from visible to near infrared wavelengths. The measured insertion loss is 0.68 dB at 1310 nm and 0.92 dB at 1550 nm, and the measured return loss is 47.8 dB at 1310 nm and is 47.67 dB at 1550 nm.

Index Terms: Optofluidics, variable optical attenuator, single-mode fiber, attenuation.

1. Introduction

Variable optical attenuators (VOAs) are widely used in sensing, signal processing, and optical communication, particularly in the wavelength-division multiplexing (WDM) system. VOAs are used to dynamically control the optical power level of light sources and the gain equalization of amplifiers, and manage the optical power in receiver front-ends to avoid overload [1], [2].

Most VOAs use microelectromechanical (MEMS) technology with shutters [3] or mirrors [4]. However, MEMS based VOAs need to use movable micromechanical elements and have difficulty integrating [5]. Some VOAs use the technologies based on liquid crystal, magneto-optic effect and electro-optic effect, but their insertion losses are often over 1 dB and have large wavelength dependent loss. Unamuno [6] proposed a MEMS based VOA with an attenuation range of 47 dB and an insertion loss of 1 dB from 1525 nm to 1565 nm. Koh and Soon [7] reported a micromirror based VOA with an attenuation range of 40 dB and an insertion loss of 1.8 dB from 1510 nm to 1610 nm. S. Rudra et al [8] utilized a blue phase liquid crystal to develop a VOA with an attenuation range of 29 dB from 1480 nm to 1550 nm.

Optofluidics, which is the combination of optics (photonics) and microfluidics, can provide VOAs some advantages such as no mechanical moving parts and miniaturization. However, there are relatively few reports about optofluidic VOAs. Most of the reported optofluidic VOAs are based on the electrowetting on dielectric (EWOD) technology. For example, Reza and Riza [9] demonstrated

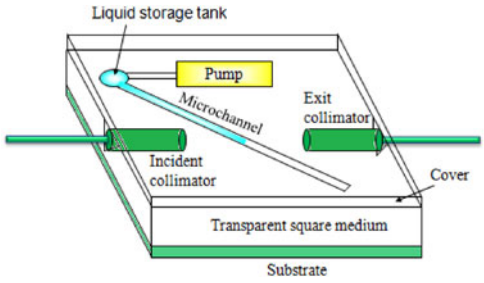

Fig. 1. Structure diagram of the VOA chip.

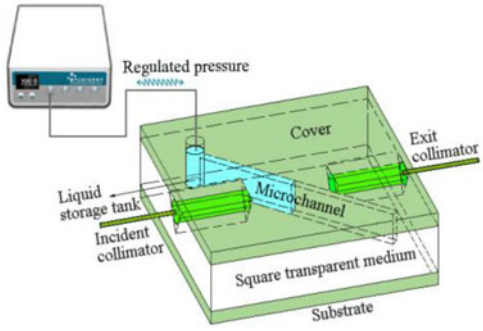

Fig. 2. VOA with a pneumatic pump.

an electrowetting-liquid-lens based VOA with an attenuation range of 40 dB and an insertion loss of 4.3 dB from 1510 nm to 1700 nm, and Dudu's *et al.* [2] reported an electrowetting based VOA which utilized a liquid drop to get the attenuation range of 26 dB from 1525 nm to 1565 nm. Also, Tang and Li [10] proposed a VOA scheme with an attenuator range of 31 dB from 1500 nm to 1600 nm by using a waveguide and a microchannel filled with fluid mixture.

Here, an optofluidic chip of the single-mode fiber VOA is proposed. It utilizes microfluid and air to regulate the optical attenuation. Its structure and working principle are simple. The VOA with this chip has a large optical attenuation range (82 dB) and a very wide operation waveband from visible to near infrared wavelengths. Here, we only discuss its single-mode characteristics at 1310 nm and 1550 nm communication wavelengths.

2. Structure and Working Principle

This VOA chip utilizes the adjustability of the fluid and regards the air column as a shutter. As shown in Fig. 1, a sandwich structure is adopted. It includes three layers: a cover, a homogeneous and transparent square medium (working layer), and a substrate. In the second layer, the incident and exit collimators are set in the V-shape grooves and their central axes lie on the same straight line; the microchannel is at the diagonal of the square medium and is connected with a liquid storage tank. Some air and liquid are sealed in the microchannel by a thin membrane, where, liquid has the same or proximal refractive index as the square medium, and air can make light all reflected. The fluid drive can use different microfluidic technologies such as electromagnetic actuation [11], [12]. Fig. 2 gives an example utilizing the air pressure actuation technology. The liquid storage tank is connected with a pneumatic pump set out of the chip. The fluid is driven by air pressure from the pump.

As shown in Fig. 3(a), when light is transmitted to the microchannel, light all falls on the solid-air interface and reflected by the "air shutter," and therefore, light energy is all attenuated. Driving liquid to arrive at the location as shown in Fig. 3(b), light all falls on the solid-liquid interface and penetrates through the microchannel into the exit collimator. There is almost no energy loss because liquid has the same or approximate refractive index as the square medium. When the air-liquid balance

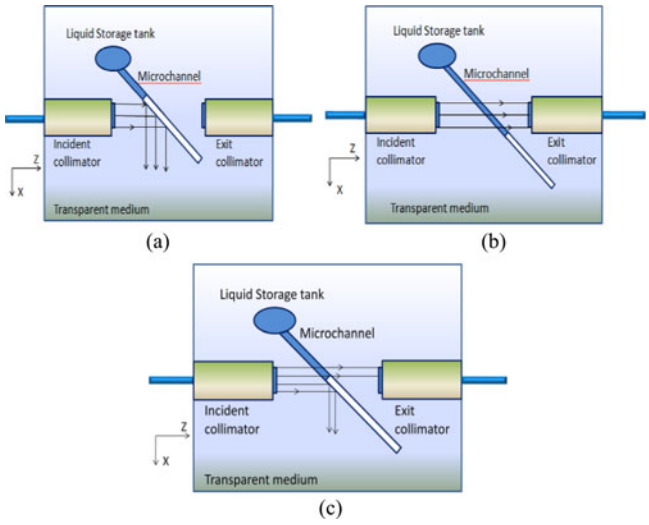

Fig. 3. Working-principle diagram of the VOA chip. (a) Light is all reflected and lost. (b) Light penetrates through the microchannel. (c) Light energy is partly attenuated.

location is as shown in Fig. 3(c), light energy is partly attenuated. So the VOA attenuation can be regulated by driving the fluid to arrive at different air-liquid balance locations in the microchannel.

This VOA chip is made of PMMA (Polymethyl methacrylate) with a refractive index of 1.49 at 589 nm. At the solid-air interface of the microchannel, the critical angle of the total reflection is between 41.5° and 42.5° within 400 nm−1700 nm, while the incident angle of light is 45°. Therefore, the total reflection condition is met, and the chip can be operated from visible to NIR wavelengths. Therefore, this VOA chip is a broadband optical device. However, different fibers and collimators are required to match the corresponding wavebands at wide waveband operations.

3. Theories

Here the optical field of the VOA chip is discussed by Gauss beam propagation theory, Helmholtz equation and coupling theory. Assuming the VOA works in the single-mode optical field, the optical wavefunction in front of the microchannel can be expressed by Gaussian beam as follows:

$$\varphi_0(x, y, z) = \frac{A_0}{\omega(z)} \exp\left(-\frac{x^2+y^2}{\omega^2(z)}\right) \exp\left\{-i\left[k\left(z+\frac{x^2+y^2}{2R(z)}\right) - \tan^{-1}\left(\frac{\lambda z}{\pi\omega_0^2}\right)\right]\right\} \tag{1}$$

where λ is the wavelength; A_0 is a constant; k is the wave vector; $\omega(z)$, ω_0 and $R(z)$ are the radius, the beam-waist radius and the wavefront curvature radius of Gaussian laser beam, respectively.

The optical field behind the microchannel includes light penetrating through the microchannel and light diffracted by the liquid head face (the air-liquid interface) in the microchannel. Referring to Fig. 3(c), assume that the origin of the coordinates is the intersection point of the optical axis and the microchannel, x coordinate value of the liquid head face is a_x. When diffraction is not considered, the optical wave penetrating the microchannel is

$$\varphi_1(x, y, z) = \begin{cases} \varphi_0(x, y, z), & x < a_x \\ 0, & x > a_x. \end{cases} \tag{2}$$

Due to diffraction at the liquid head face, the light beam behind the microchannel becomes wider, and the optical energy into the exit collimator is further reduced. This loss originated from diffraction is called the mode-field mismatch loss, and the diffraction wave meets the Helmholtz equation

$$\varphi_2(x, y, z) = \int_{-\infty}^{\infty}\int_{-\infty}^{\infty} \varphi(k_x, k_y) \exp\left\{-i\left[k_x x + k_y y + (k^2 - k_x^2 - k_y^2)^{\frac{1}{2}} z\right]\right\} dk_x dk_y \tag{3}$$

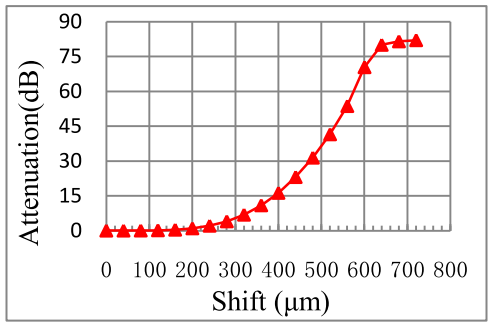

Fig. 4 Attenuation vs. fluid shift, at 1310 nm.

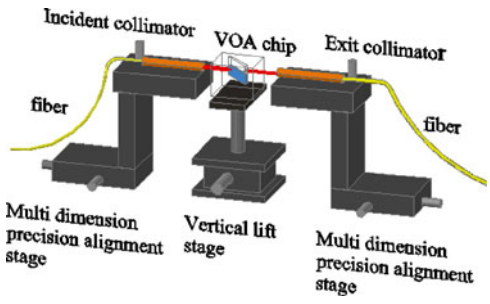

Fig. 5. Basic experimental setup.

where $k = 2\pi/\lambda$; k_x, k_y are two components of the wave vector k. By Fourier transform, integral, and simplification, (3) finally becomes as follows:

$$\varphi_2(x, y, z) = 2A_0\pi\sqrt{\pi}e^{jka_x}(1+i)\sqrt{\frac{k^2}{kz\omega_0^2 - 2iz^2}} \bullet \exp(-ikz) \bullet \exp\left(-\frac{ky^2}{k\omega_0^2 - 2iz}\right) \bullet \int_{ax}^{\infty} \exp\left(-\frac{x'^2}{\omega_0^2}\right) \exp\left[-\frac{ik}{2z}(x-x')^2\right]dx'. \quad (4)$$

The VOA attenuation includes the attenuation from the total reflection of the air shutter (IL_1) and the mode-field-mismatch attenuation from the diffraction (IL_2). According to the mode-field-coupling theory, the total attenuation (IL) is

$$IL = IL_1 + IL_2 = -10\lg\frac{\left|\iint_S \varphi_0\varphi_1 * dS\right|^2}{\iint_S|\varphi_0|^2dS \times \iint_S|\varphi_1|^2dS} - 10\lg\frac{\left|\iint_S \varphi_0\varphi_2 * dS\right|^2}{\iint_S|\varphi_0|^2dS \times \iint_S|\varphi_2|^2dS} \quad (5)$$

where φ_0, φ_1, and φ_2 are Gaussian beams, the penetrating wave, and the diffraction wave, respectively.

Assume that the wavelength is 1310 nm, the distance between the two collimators is 20 mm, and the waist radius of Gaussian beam (ω_0) is 0.25 mm. The relation between the attenuation and the fluid shift is shown in Fig. 4, where Software Mathematics is used for the theoretical calculation. The theoretical result shows the attenuation range of the proposed VOA chip is about 80 dB.

4. Experiments and Discussion

Here the optical characteristics of the proposed VOA chip are researched by principle experiments. The basic experimental setup is shown in Fig. 5. The VOA chip is made of PMMA with a dimension of 15 × 15 × 15 mm^3 (length × width × height), and the microchannel size is 10 × 1 × 4 mm^3

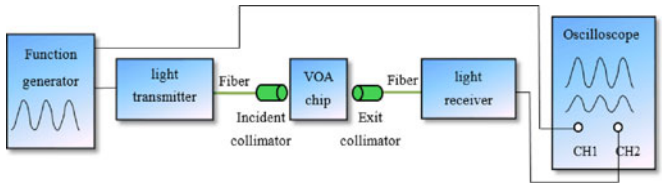

Fig. 6. Signal transmission experimental setup.

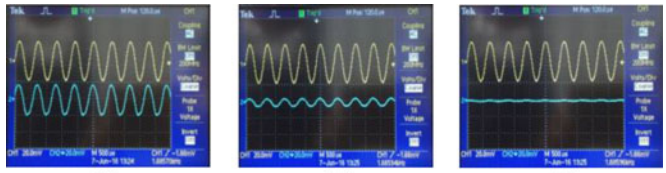

Fig. 7. Transmission of the analog signal, where the upper is the input signal, and the lower is the output signal. (a) 2.36 dB attenuation. (b) 13.05 dB attenuation. (c) 37 dB attenuation.

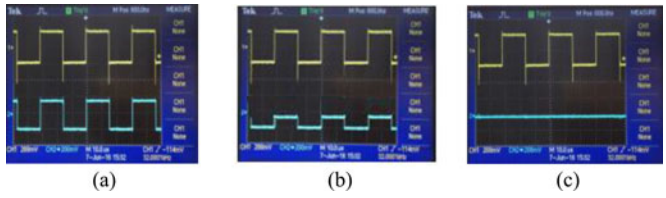

Fig. 8. Transmission of the digital signal (square wave), where the upper is the input signal, and the lower is the output signal. (a) 2.36 dB attenuation. (b) 13.05 dB attenuation. (c) 37 dB attenuation

(length $\times$ width $\times$ depth). The fabrication method uses the precision engraving technology based on a CNC engraving machine. The liquid is phenylmethylsilicone fluid with the same refractive index as PMMA. In the microchannel, air is at the upper layer, and liquid is at the lower layer. This chip is set on a vertical lift stage with 0.005 mm shifting precision. The incident and exit collimators are collimated by a pair of multi dimension precision alignment stages.

4.1 Experimental Phenomenon

Based on the basic experimental setup, the signal transmission experimental setup is shown in Fig. 6. As the chip moves down following the vertical lift stage, the liquid in the microchannel descends, and the laser beam in front of the microchannel moves gradually from the solid-liquid interface to the solid-air interface. As a result, the output signal energy attenuates. An oscilloscope is used to observe the input and output signals. The experimental photos in Figs. 7 and 8 show that the output signal becomes gradually weak as the laser beam moves from the solid-liquid interface to the solid-air interface, where the wavelength is 1550 nm.

After removing the function generator and the light transmitter in Fig. 6, connect a multi-wavelength laser to the incident collimator. Then an optical detector card is set in front of the exit collimator to observe the output laser spot of 1310 nm or 1550 nm. A visible light spot will appear on the optical detector card when the invisible near infrared (1310 nm or 1550 nm) irradiates the optical detector card. The output laser spot is captured by a CCD camera, as shown in Fig. 9. As the laser beam in front of the microchannel moves gradually from the solid-liquid interface to the solid-air interface, the output spot becomes gradually smaller and darker and finally disappears. The experiment results indicate it is feasible to regulate optical attenuation using the proposed chip.

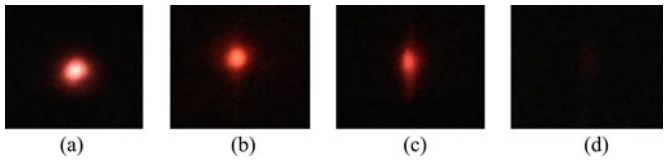

Fig. 9. Variation of the output laser spot observed by an optical detector card at 1310 nm. (a) All lasers reach the solid-liquid interface and penetrate through the microchannel. (b) Most lasers reach the solid-liquid interface and penetrate through the microchannel. (c) Half of the lasers reach the solid-liquid interface and penetrate through the microchannel. (d) Only the edge of the laser beam reaches the solid-liquid interface, and almost all of the laser is reflected off.

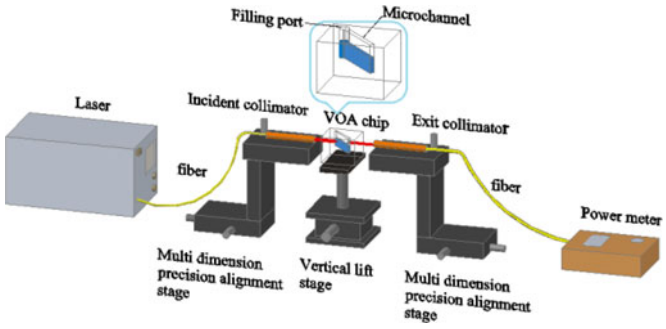

Fig. 10. Experimental setup for the attenuation measurement.

4.2 Attenuation Measurement

Based on the basic experimental setup in Fig. 5, a multi wavelength laser is connected to the incident collimator, and an optical power meter is connected to the exit collimator to detect the laser output power, as shown in Fig. 10. The laser outputted from the incident collimator has a 0.5 mm diameter. The sensitivity of the optical power meter is −82.7 dBm at 1310 nm and −83.2 dBm at 1550 nm, and its resolution is 0.01 dBm.

Fig. 11 shows the measured attenuations. As the liquid moves down and the laser beam moves gradually from the solid-liquid interface to the solid-air interface, the attenuation increases gradually. The proposed VOA chip can attenuate all optical energy in theory. However, the attenuation measurement is limited by the sensitivity of the optical power meter, so the attenuation range measured in our experiments is only 82 dB. This attenuation range has been more than that of the ordinary VOAs. Fig. 11(a) shows that the experiment data are consistent with theoretical results at the change trend. The experiment data are a bit larger than the theoretical data due to the insertion loss in the experiments. Fig. 11(b) shows that the attenuations of two optical communication wavelengths. The attenuation of 1550 nm is a bit larger than the attenuation of 1310 nm at the same liquid shift.

The insertion loss comes from the extra energy losses due to absorption of the chip material, the index mismatching of the chip material with the liquid, and offset/ angular misalignments of the two collimators. The insertion loss has different data at the different wavelength. Here the measured insertion loss is 0.68 dB at 1310 nm and 0.92 dB at 1550 nm. When all kinds of conditions are the same, the repeatability is 0.04 dB at 1310 nm and 0.05 dB at 1550 nm in terms of the attenuation versus the liquid-position.

4.3 Return Loss Measurement

The experimental setup for measuring the return loss is shown in Fig. 12. Assume that the optical power into the VOA (the output power from Port 2 of the optical circulator) is P_1, and the reflective-light power of the VOA (the output power from Port 3 of the optical circulator) is P_2. Then, the return

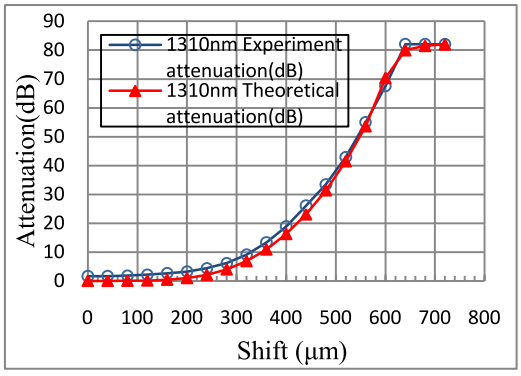

(a)

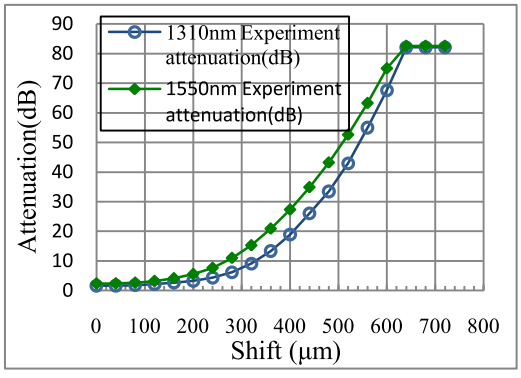

(b)

Fig. 11. Attenuation versus liquid shift. (a) Comparison between the experimental data and the theoretical data at 1310 nm. (b) Attenuations of two optical fiber communication wavelengths.

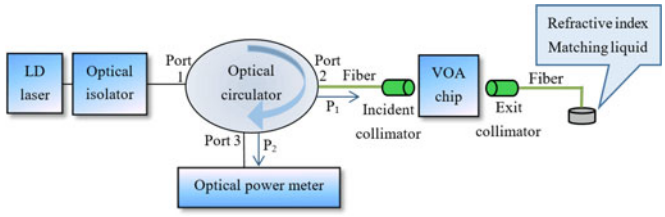

Fig. 12. Experimental setup for measuring the return loss of the VOA.

loss is as follows [13], [14]:

$$Returnloss = 10lg\frac{P_1}{P_2} - Insertloss_{2+3} \tag{6}$$

where, $Insertloss_{2+3}$ is the total of the insertion losses from Port 2 and Port 3 of the optical circulator.

At first, connect Port 2 of the optical circulator to a power meter, and read the optical power P_1 (namely, the input power of the VOA). Then, remove the power meter and connect Port 2 of the optical circulator to the incident collimator. The fiber end of the exit collimator is immerged in the matching liquid with the same refractive index as the fiber so as to avoid the effect of the end reflection. Use the power meter to measure the output power P_2 from Port 3 of the optical circulator. Finally, the return loss is obtained through (6). The experimental data of the return-loss measurement are shown in Table 1. The return loss is 47.8 dB at 1310 nm and is 47.67 dB at 1550 nm.

TABLE 1
Experimental Data of the Return-Loss Measurement

	1310nm	1550nm
P_1 (dBm)	-1.20	-1.08
P_2 (dBm)	-49.45	-49.20
$Insert\ loss_{2+3}$ (dB)	0.45	0.45
Return loss (dB)	47.8	47.67

5. Conclusion

Here, an optofluidic chip of the single-mode fiber VOA is proposed. It has a simple structure and a very wide operation waveband. It utilizes microfluid and an air shutter to regulate the optical attenuation. The single-mode characteristics are discussed at 1310 nm and 1550 nm. The experiment results indicate that it is feasible to regulate optical attenuation using the proposed chip and that the VOA chip has a large optical attenuation range (82 dB). The return loss and the insertion loss can meet the need in applications.

References

[1] A. Duduś, R. Blue, and D. Uttamchandani, "Single-mode fiber variable optical attenuator based on a ferrofluid shutter," *Appl. Opt.*, vol. 54, no. 8/10, pp. 1952–1957, Mar. 2015
[2] A. Duduś, R. Blue, M. Zagnoni, G. Stewart, and D. Uttamchandani, "Modeling and characterization of an electrowetting-based single-mode fiber variable optical attenuator," *IEEE J. Select. Top. Quantum Electron.*, vol. 21, no. 4, Jul./Aug. 2015, Art. no. 4500209.
[3] X. M. Zhang, Q. W. Zhao, A. Q. Liu, J. Zhang, J. H. Lau, and C. H. Kam, "Asymmetric tuning schemes of MEMS dualshutter VOA," *J. Lightw. Technol.*, vol. 26, no. 5, pp. 569–579, Mar. 2008.
[4] H. Cai, X. M. Zhang, C. Lu, A. Q. Liu, and E. H. Khoo, "Linear MEMS variable optical attenuator using reflective elliptical mirror," *IEEE Photon. Technol. Lett.*, vol. 17, no. 2, pp. 402–404, Feb. 2005.
[5] O. Tabata, T. Tsuchiya, O. Brand, G. K. Fedder, C. Hierold, and J. G. Korvink, Eds., *Reliability of MEMS: Testing of Materials and Devices*. Weinheim, Germany: Wiley-VCH, 2008.
[6] A. Unamuno, R. Blue, and D. Uttamchandani, "Modeling and characterization of a vernier latching MEMS variable optical attenuator," *J. Microelectromech. Syst.*, vol. 22, no. 5, 1229–1241, 2013.
[7] K. H. Koh, B. W. Soon, and J. M. Tsai, "Study of hybrid driven micromirrors for 3-D variable optical attenuator applications," *Opt. Exp.*, vol. 20, no. 19, pp. 21598–21611, 2012.
[8] G. Zhu, B. Y. Wei, and L. Y. Shi, "A fast response variable optical attenuator based on blue phase liquid crystal," *Opt. Exp.*, vol. 21, no. 5, pp. 5332–5337, 2013.
[9] S. A. Reza and N. A. Riza, "A liquid lens-based on broadband variable fiber optical attenuator," *Opt. Commun*,. vol. 282, no. 7, pp. 1298–1303, 2009.
[10] X. Tang, R. J. Li, and J. K. Liao, "A scheme for variable optofluidic attenuator: Design and simulation the corresponding," *Opt. Commun.*, vol. 305, pp. 175–179, 2013.
[11] J. Wan, Y. Zuo, Z. B. Wang, F. Yan, L. Ge, and Z. C. Liang, "Magnetohydrodynamic microfluidic drive of ionic liquids," *J. Microelectromech. Syst.*, vol. 23, no. 6, pp. 1463–1470, 2014.
[12] J. Wan, A. J. Guo, F. Yan, S. Zhang, and Z. C Liang, "A new variable optical attenuator based on microfluidics," *Acta Opt. Sinica*, vol. 34, no. 9, pp. 252–258, 2014.
[13] H. X. Zhang, "A new method for measuring the returnloss of fiber optic components," *Metrol. Meas. Technol.*, vol. 26, no. 2, pp. 42–46, 2006.
[14] 2012. [Online]. Available: http://www.doc88.com/p-997392357504.html